Optical control of intersubband absorption in a multiple quantum well-embedded semiconductor microcavity

Ansheng Liu[a] and C. Z. Ning

NASA Ames Research Center, M/S N229-1, Moffett Field, CA 94035
[a]Also at Arizona State University, Department of Electrical Engineering, Tempe, AZ 85287

ABSTRACT

Optical intersubband response of a multiple quantum well (MQW)-embedded microcavity driven by a coherent pump field is studied theoretically. The n-type doped MQW structure with three subbands in the conduction band is sandwiched between a semi-infinite medium and a distributed Bragg reflector (DBR). A strong pump field couples the two upper subbands and a weak field probes the two lower subbands. To describe the optical response of the MQW-embedded microcavity, we adopt a semi-classical nonlocal response theory. Taking into account the pump-probe interaction, we derive the probe-induced current density associated with intersubband transitions from the single-particle density-matrix formalism. By incorporating the current density into the Maxwell equation, we solve the probe local field exactly by means of Green's function technique and the transfer-matrix method. We obtain an exact expression for the probe absorption coefficient of the microcavity. For a $GaAs/Al_xGa_{1-x}As$ MQW structure sandwiched between a GaAs/AlAs DBR and vacuum, we performed numerical calculations of the probe absorption spectra for different parameters such as pump intensity, pump detuning, and cavity length. We find that the probe spectrum is strongly dependent on these parameters. In particular, we find that the combination of the cavity effect and the Autler-Townes effect results in a triplet in the optical spectrum of the MQW system. The optical absorption peak value and its location can be feasibly controled by varying the pump intensity and detuning.

Keywords: Quantum well, Intersubband transition, Semiconductor microcavity, Pump-probe spectroscopy

1. INTRODUCTION

In recent years modification of optical properties of few-level atomic systems through a strong coherent control field has attracted much attention. It has been shown that the control-field-induced quantum interference and electromagnetically induced transparency (EIT) can be utilized for enhancing conversion efficiency of sum-frequency generation,[1,2] for decreasing the threshold of switching in optical bistability,[3] for light amplification and lasing without population inversion,[4-8] and for suppression and enhancement of two photon absorption.[9] The same idea of using control lasers in manipulating the optical properties was also applied to semiconductor quantum well (QW) systems.[10-20] Compared to the atomic systems, the semiconductor nanostructures such as QW's have an advantage of feasible control of their electronic and optical properties by use of band-gap engineering. This unique feature makes these semiconductor quantum structures more attractive for optoelectronic device applications. Since semiconductor QW's are different from atomic systems in many aspects, whether one can obtain phenomena in these quantum structures similar to those of the atomic systems still remains to be explored. Previously, it was shown that the optical interband absorption of a three-subband (two conduction subbands and one valence subband) QW structure can be significantly reduced by applying a strong pump field to couple the two conduction subbands.[13,16,20] Such a reduction in the probe absorption is due to the coherent pump-probe nonlinear interaction in the QW system. Under the condition that there is a population inversion between the upper and lower conduction subbands, it was also predicted that gain without inversion (GWI) for the interband probe field is possible in the intersubband-pumped three-subband QW system.[16] Optical intersubband response of a single quantum well driven by a coherent intersubband pumping has also been discussed.[10,12,17,19] Gain with and without population inversion was predicted.[19] In the far-infrared (THz) frequency range, the optical gain due to population inversion and Raman processes in optically-pumped step quantum wells was also calculated.[21]

It has also been shown that the intersubband optical properties of quantum wells can be modified by placing them in front of a mirror[22] or inside a cavity.[23] The electromagnetic interaction between the cavity mode and

Send correspondence to A.L.: E-mail: aliu@nas.nasa.gov

intersubband spacing between the two highest-lying subbands of the QW and the probe field excites the intersubband transition between the two lower subbands (see Fig. 1). For a symmetric QW system considered in this paper, the intersubband transition between subbands 1 and 3 is electric-dipole forbidden. Moreover, it is assumed that only the first subband is thermally populated. Thus, the strong pump field essentially couples the two empty subbands. The pump beam does not induce the population redistribution among the three subbands. The local-field correction to the pump field can be neglected. However, we stress that the local-field effect for the probe field has to be taken into account because it involves a populated subband (the ground state).

In order to calculate the probe optical absorption spectrum of a MQW structure in the presence of the strong pump field, let us first derive the probe-induced current densities associated with electronic intersubband transitions for a single QW. To this end we start by writing the total Hamiltonian of the QW system coupled by a strong pump and a weak probe fields, i.e.,

$$H = H_0 + H' + H_{random} \ , \tag{1}$$

where H_0 is the light-unperturbed Hamiltonian, H' is the interaction Hamiltonian, and H_{random} is a Hamiltonian accounting for the random perturbation on the system by the thermal reservoir around the system. In the following we shall assume that the random thermal perturbation can be described in a simple relaxation-time approximation. In the gauge in which the scalar potential of the light field is zero, the interaction Hamiltonian reads as

$$H' = \frac{e}{2m^*}(\vec{p}\cdot\vec{A} + \vec{A}\cdot\vec{p}) \ , \tag{2}$$

where m^* denotes the effective mass of the electrons, and $\vec{p}$ and $\vec{A}$ are the momentum operator and the vector potential describing both the pump and probe fields, respectively. Since in this paper we are interested in the resonant optical intersubband response, we have neglected the $\vec{A}\cdot\vec{A}$ term of the interaction Hamiltonian. Due to the slab geometry of the QW structure, the local electric field, which is related to the vector potential via $\vec{E}(\omega,\vec{r}) = i\omega\vec{A}(\omega,\vec{r})$, takes the following form

$$\vec{E}(\omega,\vec{r}) = \vec{E}(\omega,z)\exp(i\vec{q}_{\|}\cdot\vec{r}_{\|}) \ . \tag{3}$$

The eigenstate of the QW system in the absence of the light field can be written as

$$|n\vec{k}_{\|}\rangle = \frac{1}{2\pi}\exp(i\vec{k}_{\|}\cdot\vec{r}_{\|})\psi_n(z) \ , \tag{4}$$

and the eigenenergy $E_n(k_{\|})$ is determined from

$$H_0|n\vec{k}_{\|}\rangle = E_n(k_{\|})|n\vec{k}_{\|}\rangle \ . \tag{5}$$

The explicit expression for H_0 in the effective-mass approximation can be found, for example, in Ref. 24. Note that, since for the highly doped QW structure considered here the conduction band nonparabolicity[24] becomes important, we have taken into the nonparabolic dispersion of the electronic subbands in the calculation of the light-induced current densities. Thus the subband separation $[E_n(k_{\|}) - E_{n'}(k_{\|})]$ in general depends on the wave vector $k_{\|}$, where $E_n(k_{\|}) = E_n + \hbar^2 k_{\|}^2/(2m^*_{\|n})$ gives the subband energy dispersion, with $m^*_{\|n}$ being the so-called parallel effective electron mass of the quantum well, which originates in the conduction band nonparabolicity effect.[24] The single-particle envelope wave functions $\psi_n(z)$ (n=1, 2, and 3)] and the corresponding energy eigenvalues [E_n (n=1, 2, and 3)] are calculated selfconsistently by solving the coupled one-band effective-mass Schrödinger equation and Poisson equation, with taking into account the exchange and correlation effects in the local density approximation.[25] Because, under usual experimental conditions, the wave number of the light is several orders of magnitude smaller than the Fermi wave number of the electron, it is reasonable to assume that the intersubband transition is vertical, namely the transition occurs at the same in-plane wave vector $\vec{k}_{\|}$. Therefore, in the representation of Eq.(4), the equations of motion for the diagonal and off-diagonal elements of the density operator can be written as

$$i\hbar\frac{\partial\rho_{nn}}{\partial t} = -\frac{i\hbar}{\tau_1}[\rho_{nn} - \rho^{(0)}_{nn}] + \sum_m (H'_{nm}\rho_{mn} - \rho_{nm}H'_{mn}) \ , \tag{6}$$

$$i\hbar\frac{\partial\rho_{nn'}}{\partial t} = \hbar[\omega_{nn'}(k_{\|}) - i/\tau_2]\rho_{nn'} + \sum_m (H'_{nm}\rho_{mn'} - \rho_{nm}H'_{mn'}) \ , \tag{7}$$

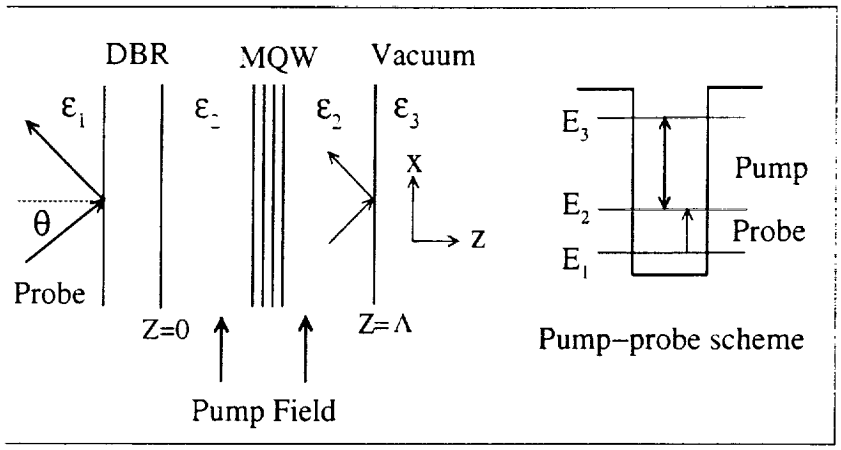

Figure 1. A schematic diagram showing the MQW-embedded microcavity excited by a pump field and probed by a weak probe field. The pump-probe level scheme is also displayed.

the electronic intersubband excitations leads to the so-called normal-mode or vacuum-field Rabi splitting of the intersubband absorption spectrum.[23] Therefore, one would expect that a combination of the cavity effect and pump field provides more feasible control of the optical properties of the quantum well system. In this paper we present a theoretical study of intersubband response of a multiple quantum well (MQW)-embedded microcavity driven by a coherent pump field. We show that the optical absorption spectra of the MQW system can be significantly modified by varying the pump intensity, detuning, and the cavity length. The fundamental framework of our theory is the Maxwell-Lorentz equation coupled with the light-induced intersubband current density. The probe-induced current density is derived from the single-particle density-matrix formalism. By using a combined Green's function and transfer-matrix method, we obtain the local field for the probe field and derive a rigorous expression for the optical absorption coefficient of the microcavity.

The present paper is organized as follows. In Sec. 2 we present the framework of our nonlocal response theory and a derivation of the probe-induced current density associated with intersubband transitions. Detailed numerical calculations of probe absorption spectra are given in Sec. 3. Finally we make a conclusion in Sec. 4.

2. THEORY

We consider a n-type doped three-subband MQW structure sandwiched between vacuum ($\varepsilon_3(\omega) = 1$) and a distributed Bragg reflector (DBR) constructed from N_m periods of two alternating component media having dielectric constants of $\varepsilon_1(\omega)$ and $\varepsilon_4(\omega)$. The DBR is limited by a semi-infinitely extended medium ε_1 serving as a prism. A schematic illustration of this MQW-embedded microcavity structure is given in Fig. 1. The barrier layers are characterized by a dielectric constant of $\varepsilon_2(\omega)$. The total quantum well number in the MQW strucure is N. In a Cartesian xyz coordinate system, it is assumed that z axis points along the direction normal to the interfaces of the QW structure, and that the DBR-medium 2 and media 2-3 boundaries are positioned at $z = 0$ and $z = \Lambda$, respectively.

Let us now consider the situation where a weak probe beam of angular frequency ω is incident at an angle θ from the prism onto the MQW structure. The angle of incidence is so chosen that the probe light is totally reflected from the barrier-vacuum interface. Thus, the strength of the Fabry-Perot microcavity effect for the probe field can be controlled by the DBR period number N_m. Furthermore, we assume that a strong pump field (also called control field) of a frequency ω_p is incident onto the MQW structure from the edge of the structure with the pump-field polarization along the well growth direction (z axis). Therefore, the cavity effect on the pump field can be neglected. The probe field is assumed to be p-polarized because we are interested in optical intersubband transitions in the QW system. Without loss of generality, we position the scattering plane of the weak probe wave in the xz plane, and the parallel (x) component of the wave vector of light thus is $q_{\|} = (\omega/c_0)\sqrt{\varepsilon_1}\sin\theta$, c_0 being the light velocity in vacuum. Futhermore, we limit our consideration to the case where the pump frequencies are in the vicinity of the

where $\omega_{nn'}(k_\parallel) \equiv [E_n(k_\parallel) - E_{n'}(k_\parallel)]/\hbar$, and τ_1 and τ_2 are phenomenological intrasubband and intersubband relaxation times, respectively. Note that in Eq.(6) $\rho_{nn}^{(0)}$ is the equilibrium diagonal element, hence the Fermi-Dirac distribution function, i.e., $\rho_{nn}^{(0)} = f_n(k_\parallel)$. For a three-subband QW system, and in the rotating-wave approximation (RWA), we solve Eqs.(6) and (7) in the frequency domain. Keeping only the resonant terms of the density matrix elements and recalling the fact that the probe beam is weak (the Rabi frequency for the probe field is almost zero), we obtain the following coupled equations

$$\hbar[\omega - \omega_{21}(k_\parallel) + i/\tau_2]\rho_{21}(\omega) = [f_1(k_\parallel) - f_2(k_\parallel)]H'_{21}(\omega) + [H'_{32}(\omega_p)]^*\rho_{31}(\omega + \omega_p) \ , \tag{8}$$

$$\hbar[\omega + \omega_p - \omega_{31}(k_\parallel) + i/\tau_2]\rho_{31}(\omega + \omega_p) = H'_{32}(\omega_p)\rho_{21}(\omega) \ . \tag{9}$$

After solving $\rho_{21}(\omega)$ from Eqs.(8) and (9), one can calculate the probe-field induced current density as follows:

$$\vec{J}(\omega, \vec{r}) = 2\int\int \frac{d^2k_\parallel}{(2\pi)^2}[\rho_{21}(\omega)\vec{\mathcal{J}}_{12}(\vec{r})] \ . \tag{10}$$

where $\vec{\mathcal{J}}$ is the current density operator, and the factor of 2 in front of the integral symbol arises from the electron spin. Noting the fact that

$$\vec{J}(\omega, \vec{r}) = \vec{J}(\omega, z)\exp(i\vec{q}_\parallel \cdot \vec{r}_\parallel) \ , \tag{11}$$

and that z component of the local electric field dominates the contribution to the intersubband current density, one obtains, after some algebraic manipulations, that the dominant component of the probe-field-induced current density is given by

$$J_z(\omega, z) = \frac{ie^2\hbar}{4\pi\omega(m^*)^2}\Phi_{12}(z)N_\omega \int [f_1(k_\parallel) - f_2(k_\parallel)]\Xi(k_\parallel)k_\parallel dk_\parallel \ , \tag{12}$$

$$\Xi(k_\parallel) = \frac{[\omega + \omega_p - \omega_{31}(k_\parallel) + i/\tau_2]}{[\omega - \omega_{21}(k_\parallel) + i/\tau_2][\omega + \omega_p - \omega_{31}(k_\parallel) + i/\tau_2] - \Omega^2} \ , \tag{13}$$

$$\Omega^2 = \frac{e^2|N_p|^2}{4(m^*\omega_p)^2} \ , \tag{14}$$

$$N_\omega = \int_{\rm QW} \Phi_{12}(z)E_z(z)dz \ , \tag{15}$$

$$N_p = E_p \int_{\rm QW} \Phi_{23}(z)dz \ , \tag{16}$$

$$\Phi_{ij}(z) = \psi_i(z)\frac{d\psi_j(z)}{dz} - \psi_j(z)\frac{d\psi_i(z)}{dz} \ . \tag{17}$$

In Eqs. (15) and (16), $E_z(z)$ and E_p are the local electrical field for the probe field across the QW and the pump field amplitude, respectively. The quantity Ω in Eq. (14) is the Rabi frequency for the pump field. The local field $E_z(z)$ will be solved from the Maxwell equation.

To calculate the probe absorption coefficient of the MQW-embedded microcavity, we incorparate the probe-induced current density in Eq. (12) into the Maxwell equation. Since there exist the direct and indirect (through the multiple reflection of light inside the cavity) electromagnetic coupling among the quantum wells in the MQW structure, the local-field spatial distribution for each quantum well has to be solved selfconsistently from the Maxwell equation. Following Ref. 23, we solve the wave equations for the MQW-embedded microcavity by using a combined transfer-matrix and Green's-function method. We then obtain the amplitude reflection, transmission, and hence absorption coefficients of the MQW structure (for the probe beam). The explicit results for the probe field absorbance are the same as those given in Ref. 23 except that $\alpha^{(m)}(\omega)$ in Eq. (24) of Ref. 23 should be replaced by

$$\frac{\mu_0 e^2\hbar}{4\pi(m^*)^2}\int [f_1(k_\parallel) - f_2(k_\parallel)]\Xi(k_\parallel)k_\parallel dk_\parallel \ . \tag{18}$$

In Sec. 3 we shall present numerical calculations of the probe absorption spectrum of a GaAs/Al_xGa_{1-x}As MQW structure subjected to a pump field. We will pay special attention to the interplay of the cavity effect and Autler-Townes effect on the probe absorption spectrum.

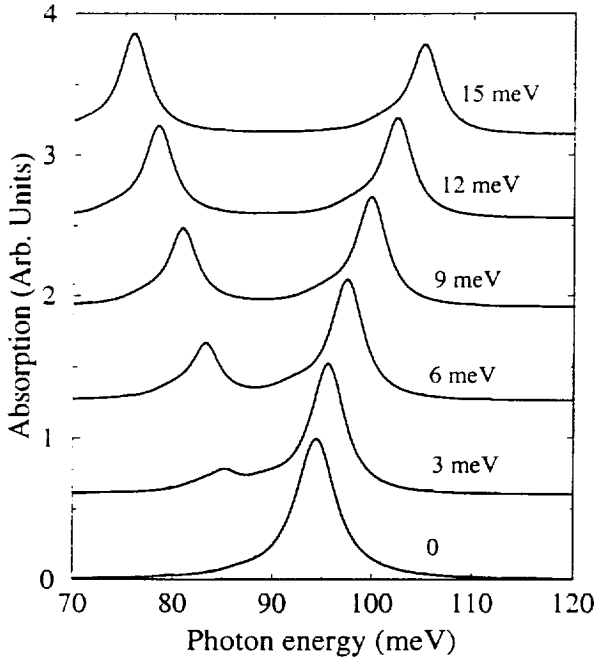

Figure 2. Probe absorption spectra of a MQW structure without the DBR for different pump intensities, i.e., $\hbar\Omega$=0, 3, 6, 9, 12, and 15 meV. The pump photon energy is $\hbar\omega_p = E_{32}(0)$=123.6 meV. For clarity, we shift the absorption spectra vertically for nonzero pump intensities.

3. NUMERICAL RESULTS AND DISCUSSION

In this section we present a numerical study of the light-controled modification in the optical properties of a MQW structure inside a microcavity. We take as a numerical example a GaAs/$Al_{0.4}Ga_{0.6}As$ MQW sandwiched between vacuum ($\varepsilon_3 = 1$) and a GaAs/AlAs DBR followed by a GaAs prism. In our calculations the following material parameters are employed: the barrier height is 318 meV, m^*=0.067m_0, $\varepsilon_1 \approx 10.9$, $\varepsilon_2 \approx 10.0$, and $\varepsilon_4 \approx 8.4$.[23] As usual, the static dielectric constant is taken to be $\varepsilon_r = 13.0$. The MQW structure is modulation doped with a sheet electron concentration of 5×10^{11} cm^{-2} per well. The well width is taken to be 100 Å. Using these parameters, we find the energy spacings between the two lowest-lying subbands of the QW and between the two upper subbands at $k_{||} = 0$ are $E_{21}(0)$=87.9 meV and $E_{32}(0)$=123.6 meV, respectively. The calculated parallel effective masses are $m^*_{||1} = 0.0725m_0$, $m^*_{||2} = 0.0841m_0$, and $m^*_{||3} = 0.101m_0$. The angle of incidence is taken to be $\theta = 55°$. The thicknesses of GaAs and AlAs layers forming the DBR are L_1=1.732 and L_4=3.147 μm, respectively. These values of the GaAs and AlAs thicknesses are so chosen that $q_{\perp 1}L_1 = q_{\perp 4}L_4 = \pi/2$ at the central frequency of 94.5 meV, where $q_{\perp 1}$ and $q_{\perp 4}$ are the perpendicular components of the light wave-vector in media 1 (GaAs) and 4 (AlAs), respectively. For the intrasubband and intersubband relaxation times, we choose $\hbar/\tau_1 = \hbar/\tau_2 = 1.5$ meV. The total number of the quantum wells used in the calculations is N=10. The distance between the adjacent quantum wells is 200 Å. In addition, we assume that the MQW is placed at the center of the cavity.

To obtain a clear understanding how the combined cavity effect and the intersubband pumping influences the probe absorption spectra of a MQW structure, it is instructive to first study separately the cavity and pump-field induced change in the probe absorption spectra. In Fig. 2 we show the pump-probe absorption spectra of the MQW system without the DBR ($N_m = 0$) (hence the cavity effect is negligibly small) at different pump intensities or Rabi frequencies, i.e. $\hbar\Omega$=0, 3, 6, 9, 12, and 15 meV. Note that the absorption coefficient calculated in this work indeed is the optical absorbance, namely, $1 - R_p - T_p$ where R_p and T_p represent the probe reflectivity and transmittance, respectively (T_p=0 in our case because the light is totally reflected from the barrier-vacuum interface, as mentioned before). The pump photon energy is $\hbar\omega_p$=123.6 meV, which is equal to $E_{32}(0)$. We see from Fig. 2 that, in the absence of the pump field, there is one resonant absorption peak appearing somewhat above the energy spacing E_{21}

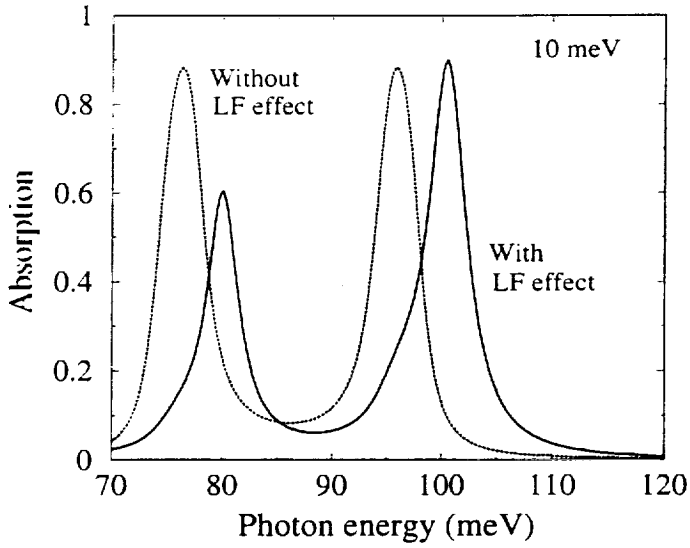

Figure 3. Comparison of probe absorption spectra of a MQW structure with and without the local-field effect. The pump Rabi frequency is $\hbar\Omega$=10 meV. The pump photon energy is $\hbar\omega_p = E_{32}(0)$=123.6 meV. The DBR period number is N_m=0.

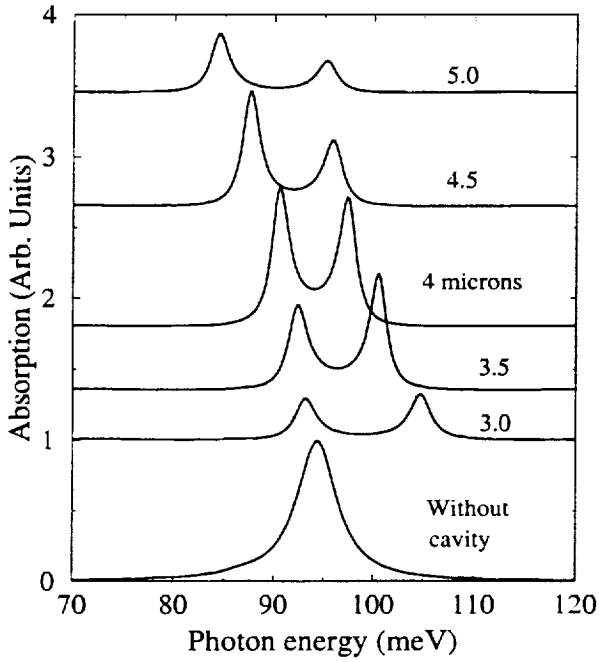

Figure 4. Absorption spectra of a MQW structure inside a cavity at different cavity lengths, i.e., Λ=3.0, 3.5, 4.0, 4.5, and 5.0 μm. The pump field is absent. The DBR period number is N_m=4. The absorption spectra at different cavity lengths are vertically shifted for clarity. The curve labelled by "Without cavity" represents the result obtained when the DBR period number is N_m=0.

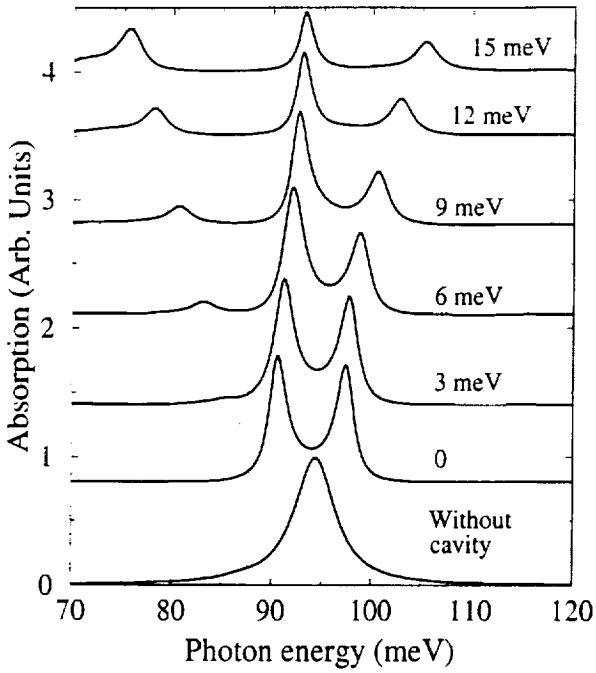

Figure 5. Probe absorption spectra of a MQW structure inside a cavity at different pump Rabi frequencies, i.e., $\hbar\Omega$=0, 3, 6, 9, 12, and 15 meV. The pump photon energy is $\hbar\omega_p$=$E_{32}(0)$=123.6 meV. For clarity, we shift the absorption spectra vertically for different pump intensities.

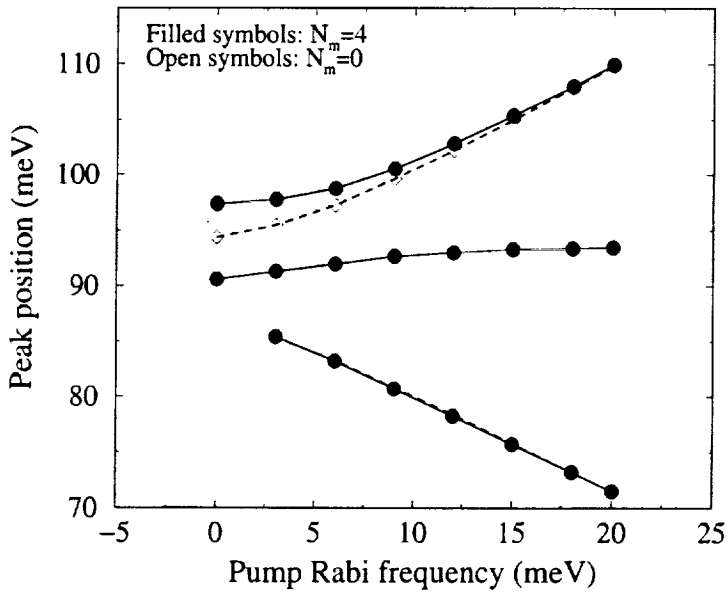

Figure 6. Peak position versus the pump Rabi frequency. The filled and open symbols represent the results with ($N_m = 4$) and without ($N_m = 0$) cavity effects, respectively. The pump photon energy is $\hbar\omega_p = E_{32}(0)$=123.6 meV.

and the FWHM width of the absorption peak is wider than $2\hbar/\tau_2$=3.0 meV used in the calculations. The blueshift of the absorption peak compared to the intersubband separation and the line-width broadening of a MQW structure are due to the local-field effect.[26] Note that the local-field blueshift of the absorption peak is also well known as the depolarization shift in the literature. We also see that the absorption spectrum is asymmetric with respect to the resonant peak because of the conduction band nonparabolicity effect. In the presence of the pump field, we see from Fig. 2 that the absorption peak is essentially splitted into two and the energy splitting becomes larger as the pump Rabi frequency is increased. This phenomenum is referred to as Autler-Townes effect that was observed in atomic systems. We also note that, when the pump Rabi frequency is small (say $\hbar\Omega$ less than 10 meV), the Autler-Townes split is quite asymmetric (the lower-energy peak is smaller than the higher-energy peak) although the pump photon energy is equal to the energy spacing $E_{32}(0)$ between the two upper subbands. To understand this result, we compare in Fig. 3 the probe spectra with and without the local-field effect in the calculations. Neglecting the local-field effect means that the local field is replaced by the external field when we calculate the absorption spectrum. Thus the local-field correction to the external field due to the quasi-two-dimensional electron gas is neglected. In the calculations of Fig. 3, we used $\hbar\Omega$=10 meV and $\hbar\omega_p = E_{32}(0)$. We see from Fig. 3 that without the local-field effect the Autler-Townes splitting is almost symmetric. (The split is not perfectly symmetric because the conduction band nonparabolicity effect slightly reduces the energy separation between the two upper subbands.) With the local-field effect taken into account, the overall spectrum is blueshifted and the lower-energy peak is obviously smaller than the higher-energy peak. Thus, it is quite clear that the asymmetric Autler-Townes splitting in Fig. 2 is mainly due to the local-field effect.

Let us now investigate the cavity effect on the absorption spectra without the pump field. In Fig. 4 we show the absorption spectra of the MQW structure inside a cavity at different cavity lengths, i.e., Λ= 3.0, 3.5, 4.0, 4.5, and 5.0 μm. For comparison, we also display the spectrum without the cavity effect. In Fig. 4 the DBR period number is N_m=4. We see from Fig. 4 that the absorption spectrum is also splitted when the cavity effect is included and the energy splitting and the peak heights of the absorption doublet are strongly dependent on the cavity length. The cavity-induced splitting is attributed to the coupling between the cavity mode and the intersubband excitation of the MQW structure.[23]

After having discussed separately the cavity and pump-field effect on the absorption spectra, we are ready to study the probe spectra when the two effects are simulatenously present. In Fig. 5 we show the probe spectra of a MQW structure inside a cavity at different pump intensities, i.e., $\hbar\Omega$ =0, 3, 6, 9, 12, and 15 meV. For comparison, we also display the absorption spectrum in the absence of both cavity and pump field, which is labelled by "Without cavity". In Fig. 5 the cavity length is Λ=4.0 μm and the DBR period number is N_m=4. The pump photon energy is $\hbar\omega_p$=123.6 meV. Fig. 5 shows that there exist three peaks in the probe spectrum when the cavity and pump field are present. The peak locations and heights are strongly dependent on the pump intensities. This triplet in the probe spectrum is due to the electromagnetic coupling between the cavity mode and Autler-Townes splitted intersubband resonances. In Fig. 6 we compare the peak position dependence of the pump Rabi frequency with (filled symbols) and without (open symbols) the cavity effect. We see from Fig. 6 that the cavity effect mainly influences the highest-energy peak. At low pump intensities there is an obvious difference between the results with and without the cavity effect. However, as the pump Rabi frequency is increased, the difference becomes smaller. For the lowest-energy peak, the results with and without the cavity effect are very close even when the pump field is weak. The central peak is related to the cavity resonance. Owing to the interplay of the Autler-Townes effect and the cavity effect, the position of the cavity-related peak is also dependent on the pump intensity, as shown in Fig. 6.

From the application point of view, it is interesting to see how the probe absorption is controled by the pump field. In Fig. 7 we show the pump intensity dependence of the probe absorption of a MQW structure inside a cavity at different probe photon energies, i.e., $\hbar\omega$=90, 95, and 100 meV. As in Fig. 5, the cavity length is Λ=4.0 μm and the DBR period number is N_m=4. The pump photon energy is $\hbar\omega_p$=123.6 meV. We see from Fig. 7 that the pump field can either reduce or enhance the probe absorption, depending upon the probe frequency.

Finally we study the pump detuning on the pump-probe absorption spectra of a MQW structure inside a cavity. In Fig. 8 we show the probe spectra at different pump detunings, i.e., $\hbar\omega_p - E_{32}(0)$=-10, -5, 0, and 5 meV. The pump Rabi frequency is $\hbar\Omega$=15 meV. It seems from Fig. 8 that the pump detuning has a strong influence on the sidebands but a rather weak effect on the central peak. This is because the sidebands are related to the Autler-Townes doublet and the central peak is mainly determined by the cavity resonance. Owing to the mutual coupling, however, the three peaks are dependent on the pump detuning.

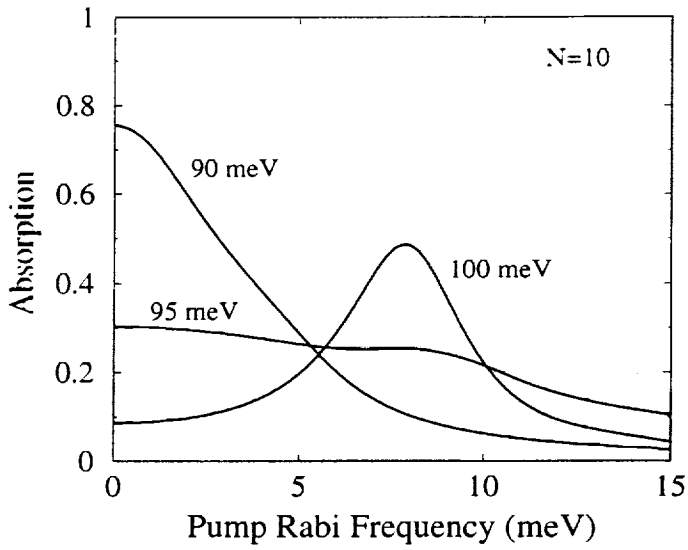

Figure 7. Probe absorption of a MQW structure inside a cavity as a function of the pump Rabi frequency at different probe photon energies. i.e., $\hbar\omega$=90, 95, and 100 meV. The pump photon energy is $\hbar\omega_p = E_{32}(0)$=123.6 meV.

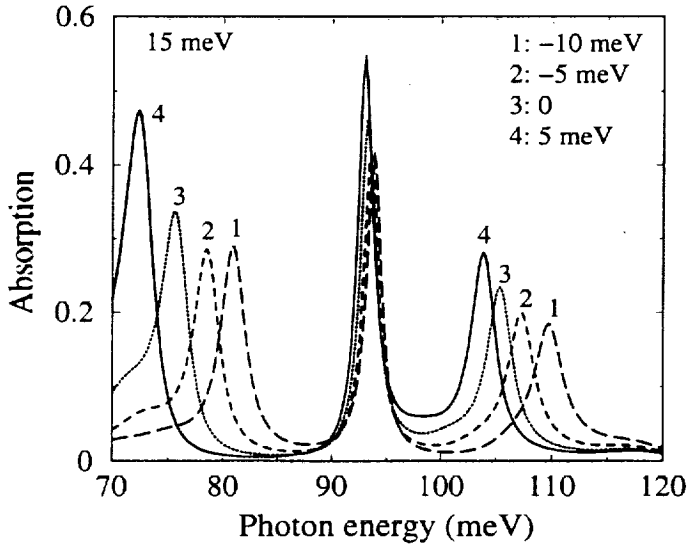

Figure 8. Probe absorption spectra of a MQW structure inside a cavity at different pump detunings, namely $\hbar\omega_p - E_{32}(0)$=-10, -5, 0, and 5 meV. The pump Rabi frequency is $\hbar\Omega$=15 meV.

4. CONCLUSION

In a nonlocal field theory, we have studied the probe optical intersubband response of a multiple quantum well-embedded microcavity driven by a coherent pump field. For a three-subband QW system, we derive the probe-induced current density associated with intersubband transitions from the single-particle density-matrix formalism. By incorporating the current density into the Maxwell equation, we solve the probe local field exactly by use of a combined Green's function and transfer-matrix method. For a GaAs/$Al_xGa_{1-x}As$ MQW structure sandwiched between a GaAs/AlAs DBR and vacuum, we performed numerical calculations of the probe absorption for different parameters such as pump intensity, pump detuning, and cavity length. We find that the combination of the cavity effect and the Autler-Townes effect results in a triplet in the optical spectrum of the MQW system. The pump field provides a feasible control of the optical absorption peak value and its location.

ACKNOWLEDGMENTS

This work is partly supported by NASA Ames Research Center Director's Discretionary Fund.

REFERENCES

1. S. E. Harris, J. E. Field, and A. Imamoglu, "Nonlinear optical processes using electromagnetically induced transparency," *Phys. Rev. Lett.* **64**, pp. 1107–1110, 1990.
2. G. Z. Zhang, M. Katsurgawa, K. Hakuta, R. I. Thompson, and B. P. Stoicheff, "Sum-frequency generation using strong-field coupling and induced transparency in atomic hydrogen," *Phys. Rev. A* **52**, pp. 1584–1593, 1995.
3. W. Harshawardhan and G. S. Agarwal, "Controlling optical bistability using electromagnetical-field-induced transparency and quantum interferences," *Phys. Rev. A* **53**, pp. 1812–1817, 1996.
4. A. Imamoglu, J. E. Field, and S. E. Harris, "Lasers without inversion: A closed lifetime broadened system," *Phys. Rev. Lett.* **66**, pp. 1154–1156, 1991.
5. A. Nottelmann, C. Peters, and W. Lange, "Inversionless amplification of picosecond pulse due to zeeman coherence," *Phys. Rev. Lett.* **70**, pp. 1783–1786, 1993.
6. E. S. Fry, X. Li, D. E. Nikonov, G. G. Padmabandu, M. O. Scully, A. V. Smith, F. K. Tittel, C. Wang, S. R. Wilkinson, and S.-Y. Zhu, "Atomic coherence effects within the sodium d_1 line: Lasing without inversion via population trapping," *Phys. Rev. Lett.* **70**, pp. 3235–3238, 1993.
7. W. E. van der Veer, R. J. van Diest, A. Donszelmann, and H. B. van Linden van den Heuvell, "Experimental demonstration of light amplification without population inversion," *Phys. Rev. Lett.* **70**, pp. 3243–3246, 1993.
8. A. S. Zibrov, M. D. Lukin, D. E. Nikonov, L. Hollberg, M. O. Scully, V. L. Velichansky, and H. G. Robinson, "Experimental demonstration of laser oscillation without population inversion via quantum interference in rb," *Phys. Rev. Lett.* **75**, pp. 1499–1502, 1995.
9. G. S. Agarwal and W. Harshawardhan, "Inhibition and enhancement of two photon absorption," *Phys. Rev. Lett.* **77**, pp. 1039–1042, 1996.
10. Y. Zhao, D. Huang, and C. Wu, "Electric-field-induced quantum coherence of the intersubband transition in semiconductor quantum wells," *Opt. Lett.* **19**, pp. 816–819, 1994.
11. A. Imamoglu and R. J. Ram, "Semiconductor lasers without population inversion," *Opt. Lett.* **19**, pp. 1744–1746, 1994.
12. D. Huang, C. Wu, and Y. Zhao, "Coulomb and light-induced electronic renormalization in quantum wells for electromagnetically induced transparency and light amplification without inversion," *J. Opt. Soc. Am. B* **11**, pp. 2258–2265, 1994.
13. D. S. Lee and K. J. Malloy, "Analysis of reduced interband absorption mechanism in semiconductor quantum wells," *IEEE J. Quantum Electron.* **QE-30**, pp. 85–92, 1994.
14. Y. Zhao, D. Huang, and C. Wu, "Field-induced quantum interference in semiconductor quantum wells for lasing without inversion and electromagnetically induced transparency," *J. Nonlin. Opt. Phys. Mater.* **4**, pp. 261–282, 1995.
15. J. B. Khurgin and E. Rosencher, "Practical aspects of lasing without inversion in various media," *IEEE J. Quantum Electron.* **QE-32**, pp. 1882–1896, 1996.
16. D. S. Lee and K. J. Malloy, "Gain without inversion in interband transitions of semiconductor quantum wells from a single-particle perspective," *Phys. Rev. B* **53**, pp. 15 749–15 755, 1996.

17. A. Liu, "Light control of optical intersubband absorption and amplification in a quantum well inside a cavity," *Phys. Rev. A* **56**. pp. 3206–3212, 1997.
18. A. Neogi. Y. Takahashi. and H. Kawaguchi, "Analysis of transient interband light modulation by ultrashort intersubband resonant light pulses in semiconductor quantum wells," *IEEE J. Quantum Electron.* **QE-33**. pp. 2060–2070, 1997.
19. A. Liu, "Self-consistent theory of optical gain with and without inversion in semiconductor quantum wells," *J. Opt. Soc. Am. B* **15**, pp. 1741–1748. 1998.
20. A. Liu and C. Z. Ning, "Exciton absorption in semiconductor quantum wells driven by a strong intersubband pump field," *J. Opt. Soc. Am. B* . in press.
21. A. Liu and C. Z. Ning, "Terahertz optical gain based on intersubband transitions in optically pumped semiconductor quantum wells: Coherent pump-probe interactions," *Appl. Phys. Lett.* **75**, pp. 1207–1209, 1999.
22. A. Liu, "Radiative interaction and disorder effect in the linear optical response of a multiple-quantum-well structure," *Phys. Rev. B* **55**, pp. 7796–7803, 1997.
23. A. Liu, "Rabi splitting of the optical intersubband absorption line of multiple quantum wells inside a fabry-perot microcavity," *Phys. Rev. B* **55**, pp. 7101–7109, 1997.
24. U. Ekenberg, "Nonparabolicity effects in a quantum well: Sublevel shift, parallel mass, and landau levels," *Phys. Rev. B* **40**, pp. 7714–7726, 1989.
25. O. Gunnarsson and B. I. Lundqvist, "Exchange and correlation in atoms, molecules, and solids by the spin-density-functional formalism," *Phys. Rev. B* **13**, pp. 4274–4298, 1976.
26. A. Liu, "Local-field effect on the linear optical intersubband absorption in multiple quantum wells," *Phys. Rev. B* **50**, pp. 8569–8576, 1994.